IEEE Access
Multidisciplinary | Rapid Review | Open Access Journal

Received April 27, 2017, accepted June 23, 2017, date of publication July 5, 2017, date of current version July 31, 2017.

Digital Object Identifier 10.1109/ACCESS.2017.2723541

Comparison of an ANFIS and Fuzzy PID Control Model for Performance in a Two-Axis Inertial Stabilized Platform

FENG LIU[1], HUA WANG[1], QINGLI SHI[1], HENGXIAN WANG[1], MENGYING ZHANG[1], AND HAILONG ZHAO [2]

[1]Department of School of Astronautics, Beihang University, Beijing 100191, China
[2]System Design Institute of Hubei Aerospace Technology Academy, Hubei 430040, China

Corresponding author: Feng Liu (lfjssx@126.com)

ABSTRACT An adaptive neuro-fuzzy inference system (ANFIS) of soft computing is an effective method for predicting performance. An statistical analysis and soft computing scheme based on the ANFIS neuro-fuzzy proportional-integral-differential (ANFP) control is proposed to predict the performance of a fuzzy PID controller for a two-axis inertially stabilized platform system. The data are extracted from an unconventional fuzzy PID stabilization controller output of the closed loop, and the model is trained using the Levenberg–Marquardt (LM) training algorithm and compared according to the experimental data from the output results of the ANFP controller. The comparative simulations are expatiated by the statistical values of the mean squared error (MSE) and the coefficient of determination (R) as performance indicators. The experimental results validate that the ANFP soft computing approach contributes to the indispensable improvement for predicting performance in accordance with the error analysis results.

INDEX TERMS Adaptive neuro-fuzzy inference system, fuzzy-PID controller, fuzzy PID, MSE value, inertial stabilized platform.

I. INTRODUCTION

An inertially stabilized platform is applied to maintain the line of sight (LOS) stabilized by external disturbances in the inertial space [1]. The stabilization controller of an intelligent approach serves a positive role in the complex and nonlinear system; thus, so most researchers concentrate on the high-performance controller.

The influence of LOS disturbances and sensor noise on the stabilization control loop was investigated [2]. The kinematics and dynamical models of the pitch/roll two-axis strap-down stabilization platform was proposed in order to satisfy the requirements of the missile seeker, and the effectiveness of the proposed method was validated [3]. A decoupling control method was presented to solve the coupling problem for the inertially stabilized platform, and the performance was improved according to the suppressing coupling factors [4], [5]. A novel method that is based on a steady-state error response was developed to identify the LuGre friction parameters and reduces the impact of nonlinear friction on the dynamic performance of the two-axis inertial stabilized platform [6]. The robust proportional integral (PI) control scheme and linear quadratic Gaussian (LQG)/loop transfer recovery (LTR) were proposed and simulated to achieve high performance and high stabilization precision for the LOS stabilization system [7], [8]. A fuzzy control scheme was adopted to improve the performance of the proposed controlled system [9]–[11]. The fuzzy control system was performed; the comparisons results indicated that the fuzzy logic controller completely reduced overshoot and steady-state errors [12]–[15]. A novel study of the ANFIS technique was formulated, and the results were analysed by employing the root mean squared error (RMSE), and the coefficient of determination (R2). The simulation results indicate that the prediction capabilities of applying the ANFIS soft computing approach yielded to significant improvement [16]. A randomized adaptive neuro-fuzzy inference system (RANFIS) was proposed for predicting the parameters; the experimental results validate the improved performance of the machine [17], [18]. A complex time series adaptive network-based fuzzy inference system that is centered around empirical mode decomposition was proposed to forecast stock prices. The results indicate that the proposed

model is superior to the other models [19]. A novel control approach of hybrid neuro-fuzzy (HNF) for load frequency control (LFC) of a four-area power system was presented, and a performance evaluation was performed by using fuzzy, ANN, ANFIS and conventional PI and PID control approaches [20], [21]. A model identification using neural networks (NN) and ANFIS for the nonlinear systems in series was proposed and designed according to the conductivity as a measured parameter and the flow rate as the manipulated variable. Real-time experimental data of the nonlinear system were employed to train the neural network by a back-propagation training algorithm and ANFIS using MATLAB [22]. Soft computing approaches are concerned with the integration of artificial intelligent intelligence tools (neural networks), fuzzy technology, evolutionary algorithms for handling the modelling and control of complex systems [23]. However, there are few studies have addressed of the controller performance based on an ANFIS control system for the inertially stabilized platform.

Motivated by the previous aforementioned discussions, in this study, the feasibility of the ANFP controller for prediction ability is proposed. The main contributions of this paper are listed as follows:

(1) The Soft computing based on the ANFP control scheme is proposed to predict the controller performance of a two-axis inertially stabilized platform system, which is the most breakthrough scheme for predicting performance for the overall control system.

(2) Membership functions (MFS) of the fuzzy PID control model develops the following unconventional hybrid functions: the Zmf and Trapmf.

(3) The improvement of the proposed ANFP optimization scheme outperforms the approach of conventional fuzzy PID control.

(4) The proposed ANFP control method expands the research directions.

The remainder of this paper is organized as follows. In Section 2, the control system is constructed. In Section 3, the motor model is formulated. In Section 4, the control schemes are proposed. Comparative simulations and tests of the proposed control approaches are expatiated in Section 5. Conclusions are depicted in Section 6.

II. CONTROL SYSTEM

Fig.1 depicts the ANFP control system, which includes the stabilized controller and the controlled object. The ANFP control scheme is an important part of the total system.

III. THE MOTOR MODEL

Based on Fig. 2, the transfer function of motor and load is expressed as follows:

$$\frac{w_m(s)}{U(s)} = \frac{C_m}{(R+Ls)\cdot Js + C_m \cdot K} \tag{1}$$

where $U(s)$ is the motor armature voltage, R is the equivalent resistance of the motor armature, L is the equivalent total inductance of the armature, J is the rotational inertia of the motor, K is the back-EMF coefficient, C_m is moment coefficient of the motor, and $w_m(s)$ is the angular velocity of the motor rotation shaft.

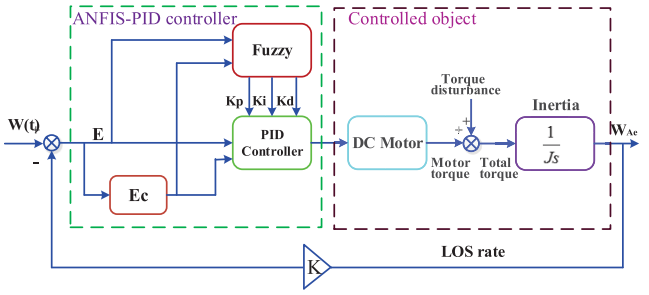

FIGURE 1. Block diagram of ANFIS fuzzy PID control system.

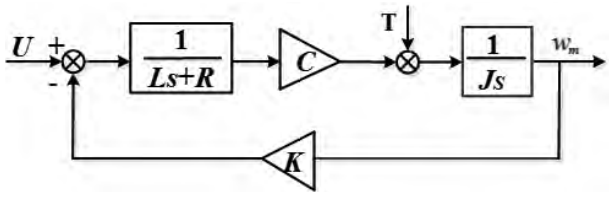

FIGURE 2. The block diagram of motor and load.

IV. CONTROL SCHEMES

A. PID CONTROL

PID is a linear controller; their control deviation is the difference between the given value $y_d(t)$ and the actual output value $y(t)$.

$$error(t) = y_d(t) - y(t) \tag{2}$$

The control law is:

$$u(t) = k_p\left[error(t) + \frac{1}{T_1}\int_0^t error(t)dt + T_D \cdot derror(t)/dt\right] \tag{3}$$

Its transfer function is as follows:

$$G(s) = \frac{U(s)}{E(s)} = k_p \cdot \left(1 + \frac{1}{T_s \cdot s} + T_D \cdot s\right) \tag{4}$$

where k_p is the proportionality coefficient, T_1 represents the integration time constant, and T_D is the differentiating time constant.

B. FUZZY LOGIC CONTROL

Fuzzy logic control primarily contains three parts: fuzzification, fuzzy inference and defuzzification.

- Fuzzification

Fuzzification is actually an input interface of the fuzzy controller, which determines the input position deviation E and the rate of change EC of the position deviation and transforms them into fuzzy quantities. Fuzzy control includes Gaussmf, gbellmf, trimf, zmf and so on in fuzzy control.

However, the trapmf, zmf and the hybrid scheme of trapmf combined with zmf are applied, and their expressions are as follows:

- Trapezoidal-shaped Membership Function (Trapmf)

The trapezoidal curve is a function of the vector x and depends on the four scalar parameters a, b, c and d, as given by the following:

$$f(x; a, b, c, d) = \begin{cases} 0, & x \le a \\ \dfrac{x-a}{b-a}, & a \le x \le b \\ 1, & b \le x \le c \\ \dfrac{d-x}{d-c}, & c \le x \le d \\ 0, & d \le x \end{cases} \quad (5)$$

Greater campacity is as follows:

$$f(x; a, b, c, d) = \max\left(\min\left(\frac{x-a}{b-a}, 1, \frac{d-x}{d-c}\right), 0\right) \quad (6)$$

The parameters a and b locate the "feet" of the trapezoid, and the parameters b and c locate the "shoulders" of the trapezoid.

- Z-shaped Membership Function (Zmf)

This spline-based function of x is named for its Z-shape. The parameters a and b locate the extremes of the sloped portion of the curve as given by the following:

$$f(x; a, b) = \begin{cases} 1, & x \le a \\ 1 - 2\left(\dfrac{x-a}{b-a}\right)^2, & a \le x \le \dfrac{a+b}{2} \\ 2\left(\dfrac{x-a}{b-a}\right)^2, & \dfrac{a+b}{2} \le x \le b \\ 0, & x \ge b \end{cases} \quad (7)$$

- Gaussian curve membership function (Gaussmf)

The symmetric Gaussian function depends on the two parameters σ and c, as given by the following:

$$f(x; \sigma, c) = e^{\frac{-(x-c)^2}{2\sigma^2}} \quad (8)$$

The parameters for Gaussmf represent the parameters σ and c listed in order in the vector [sig c].

- Fuzzy inference

Numerous fuzzy conditional statements constitute a fuzzy rule base, such as "if (E is NB) and (EC is NB) then (U is NB)", "if (E is NB) and (EC is NM) then (U is PB)", "if (E is NB) and (EC is NS) then (U is PB)", "if (E is PB) and (EC is PM) then (U is PB)" and "if (E is PB) and (EC is PB) then (U is PB)". The antecedent of a conditional sentence is the input and state, and the consequent of a conditional sentence is the control variable.

- Defuzzification

The results are expressed by the language variable when the fuzzy inference is the end; the results of language variables must be converted to an actual value in order to utilize these variables. This above process is referred to as defuzzification. Conventional schemes are centroid, mom, lom for solving the defuzzification are centroid, mom, and lom, whereas the bisector is utilized in the proposed fuzzy controller. The bisector approach is regarded as the median of $\mu_{c'}(z)$ which is the defuzzification of z, that is, $z_0 = df(z) = \mu_{c'}(z)$; the expression is as follows:

$$\int_a^{z_0} \mu_{c'}(z)\, dz = \int_{z_0}^{b} \mu_{c'}(z)\, dz \quad (9)$$

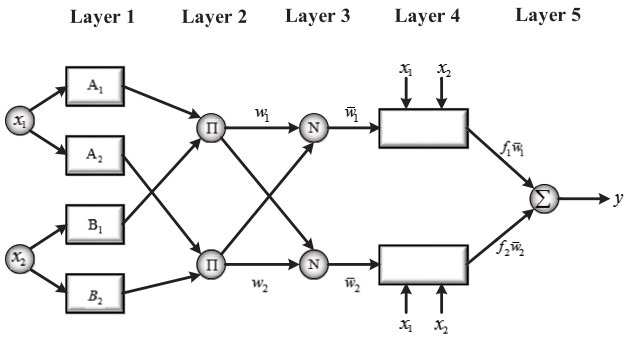

FIGURE 3. ANFIS architecture.

- Fuzzy-PID control

The deviation E and deviation rate EC of the input PID regulator are input into the fuzzy controller; the k_p, k_i and k_d are adjusted by three fuzzy controllers respectively; then, the process of fuzzifications, approximate reasons and clarifications are respectively occurred, and the revised k_p, k_i and k_d are obtained and put into the PID regulator, which are online real-time corrected.

The optimal fuzzy sets and fuzzy rule-bases, however, depend on the performance of a fuzzy-PID, which is a symbol of a human experts interpretation of linguistic variables. The control signal and closed-loop responses are affected due to the transformation of different membership functions transformation. The fuzzy sets and rule-bases of a fuzzy PID control system are automatically decided according to the optimization performance of the fuzzy PID control technology.

C. ADAPTIVE NEURO-FUZZY INFERENCE SYSTEM (ANFIS) ARCHITECTURE

The structure of ANFIS is shown in Fig.3. The Sugeno-type fuzzy inference rules are applied. This study includes forty-nine and fifty-six rules of the proposed ANFIS in this work. Two rules and the five layers are researched. The structure of ANFIS in MATLAB is depicted in Fig.4.

- Rule 1

If x is A_1 and y is B_1, then $f_1 = p_1 x + q_1 y + r_1$.

- Rule 2

If x is A_2 and y is B_2, then $f_2 = p_2 x + q_2 y + r_2$. where p_1, q_1, r_1 and p_2, q_2, r_2 are the consequent parameters. A_1, B_1 and A_2, B_2 are the linguistic labels.

- Layer 1: Fuzzification layer

$$O_{1,i} = \mu_{A_i}(x) \quad (10)$$

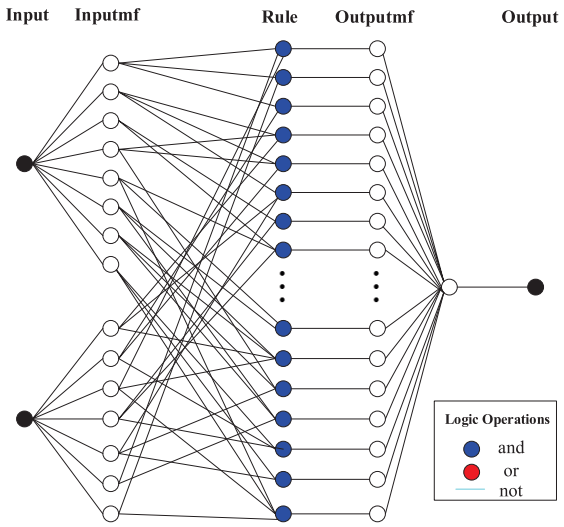

FIGURE 4. Structure of ANFIS in MATLAB.

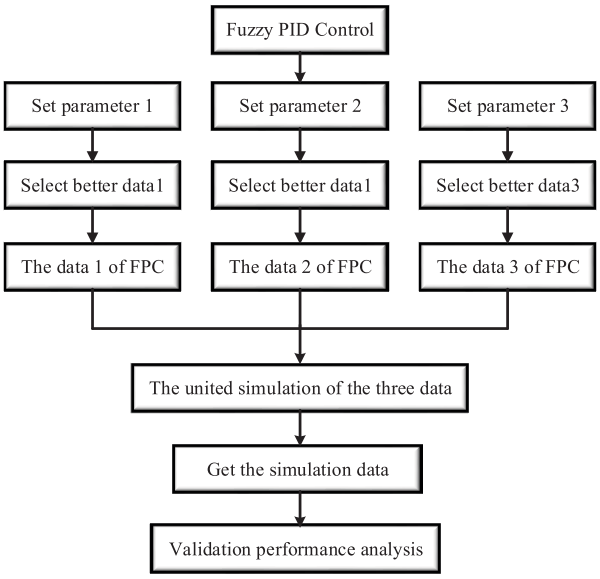

FIGURE 5. ANFIS optimization scheme.

where $O_{1,i}$ represents the output of the i node, and $\mu_{A_i}(x)$ is a Gaussian membership function (MF), that is presented according to the following relations.

$$\mu_{A_i}(x) = \exp\left[-\left(\left(\frac{x - c_i}{a_i}\right)^2\right)^{b_i}\right], \quad for\ i = 1, 2 \quad (11)$$

where a_i is the center of MF, b_i is a premise parameter of MF, and c_i denotes the width of MF, which determines the position and the shape of every membership function.

- Layer 2: Rule layer

Every node represents a fuzzy rule, which can match the antecedent of a fuzzy rule and compute the relevant grade of every rule.

$$O_{2,i} = \omega_i = \mu_{A_i}(x) \times \mu_{B_i}(x), \quad for\ i = 1, 2 \quad (12)$$

where $O_{2,i}$ denotes the output result in this layer, and ω_i represents the firing strength the i rule.

- Layer 3: Normalization layer

$$O_{3,i} = \bar{\omega}_i = \frac{\omega_i}{\omega_1 + \omega_2}, \quad for\ i = 1, 2 \quad (13)$$

- Layer 4: Defuzzification layer

$$O_{4,i} = \bar{\omega}_i f_i = \bar{\omega}_i (p_i x + q_i y + r_i), \quad for\ i = 1, 2 \quad (14)$$

- Layer 5: Output layer

$$O_{5,i} = \sum_i \bar{\omega}_i f_i = \frac{\sum_i \omega_i f_i}{\sum_i \omega_i}, \quad for\ i = 1, 2 \quad (15)$$

- The process of the optimal scheme

The process of the ANFIS is shown in Fig.5. Three steps are illustrated as follows:

Step 1: The algorithm is presented based on three comparative simulations. In the first group, three diverse parameters k_p, k_i and k_d are adjusted by simulation analysis. The best performance is employed and signed as data 1. Similarly, the data 2 of the second group is proposed; the data 3 of the third group is selected.

Step 2: Using the data 1, data 2 and data 3 as training data, the novel Gaussmfs are generated, including the membership functions and diverse rules. The excellent result is employed according to the comparative simulations.

Step 3: The co-simulation of the second step is performed, the fuzzy-PID results are obtained, and the best performance is established.

- Training data 1

The outputs of fuzzy PID control are obtained by three groups comparative simulations; the best result is selected as the first data. The comparisons of the three fuzzy PID controllers in training data 1 are presented in Fig.6; the structure of the fuzzy PID control training data is shown in Fig.7.

- Training data 2

The simulation results of fuzzy PID control are utilized by three comparative tests; the excellent results are modelled as the second data. The comparisons of three fuzzy PID controllers of training data 2 are illustrated in Fig.8; the structure of fuzzy PID control training data is shown in Fig.9.

- Training data 3

The simulation results of fuzzy PID control are utilized by three simulation tests. The best results are selected as the second data. The comparisons of the three fuzzy PID controllers in training data 3 are illustrated in Fig.10, and the structure of the fuzzy PID control training data is shown in Fig.11.

- Training data 4

The best three groups of the fuzzy PID models are obtained by the Simulink tool. The comparisons of the fuzzy PID model, PID model and two ANFP controllers, and the results

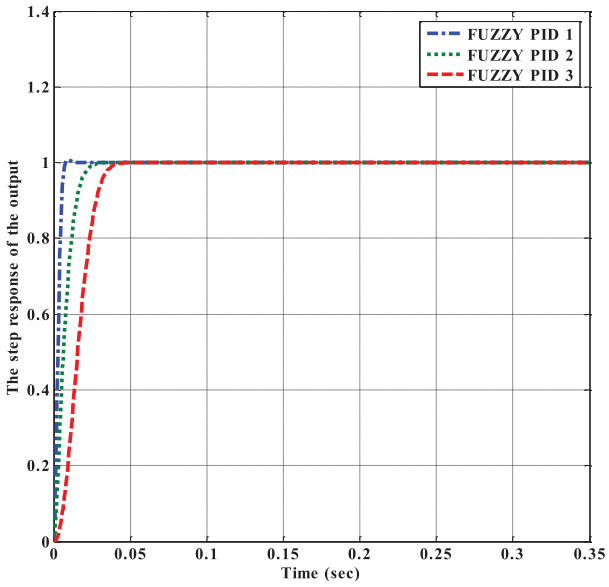

FIGURE 6. Comparison of three fuzzy PID controller of Training data 1.

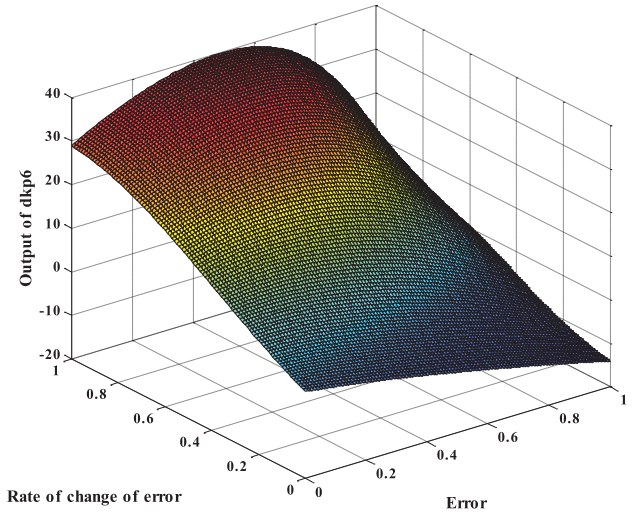

FIGURE 7. The structure of fuzzy PID control of training data 1.

TABLE 1. The comparison of three controllers performance.

Controller	Overshoot(%)	Rise time(s)	Settling time(s)
PID controller	93	0.00617	0.971
Fuzzy-PID controller	88.3	0.0107	0.976
ANFP controller	77.1	0.00249	0.878

of training data 4 are shown in Fig.12. The optimal construction type is depicted as in Fig.13. The comparative results are illustrated in Table 1.

V. SIMULATION TEST

The ANFP model design for the prediction of the output is depicted in Fig.14. Firstly, the validation, training and testing

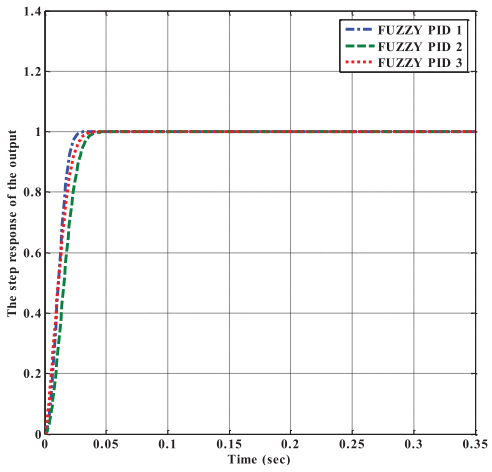

FIGURE 8. Comparison of three fuzzy PID controllers of training data 2.

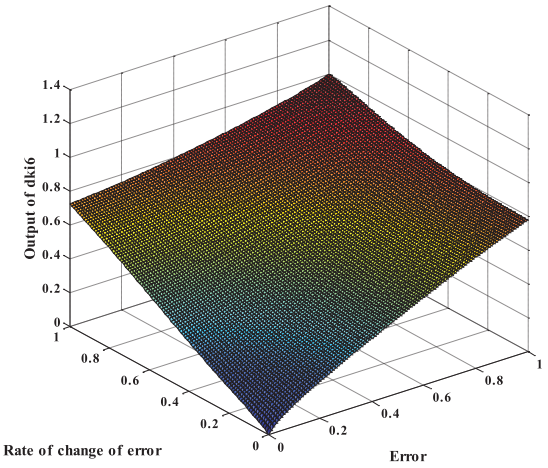

FIGURE 9. The structure of fuzzy PID control of training data 2.

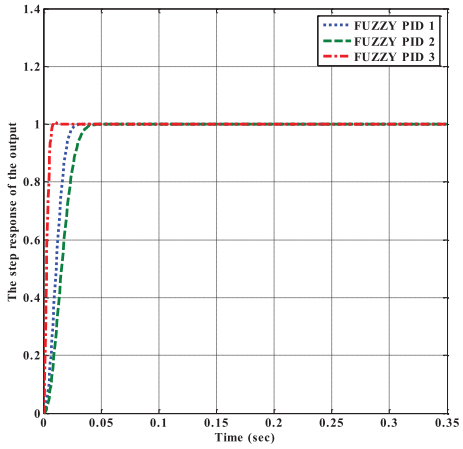

FIGURE 10. Comparison of three fuzzy PID controllers of training data 3.

data of the experimental samples are selected according to a certain proportion. Secondly, the model is built, trained and tested. Third, the next process is going to carry out if a validation is performed to determine whether the requirements are satisfied. Last but not least, the model is optimized,

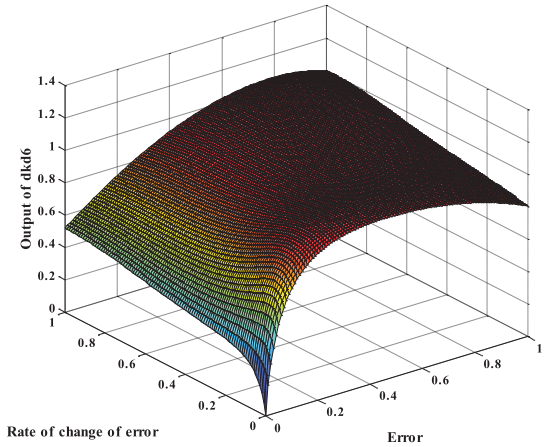

FIGURE 11. The structure fuzzy PID control of training data 3.

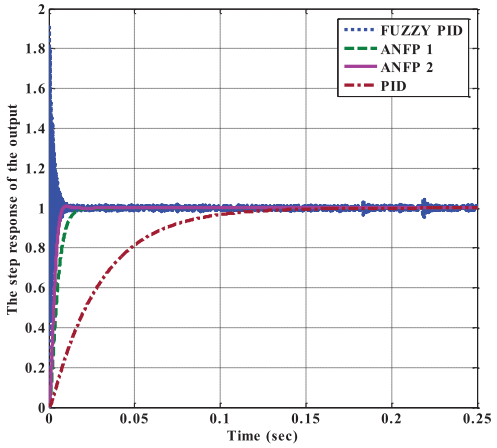

FIGURE 12. Comparison of hyprid controllers of training data 4.

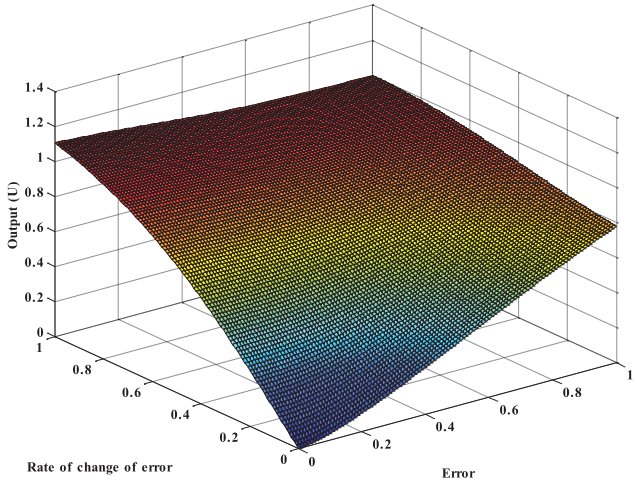

FIGURE 13. The structure of hyprid control of training data 4.

the optimal model is tested, and the results are predicted and the errors are analyzed.

The data of the last simulation are regarded as the inputs, and the part is regarded as the targets, which are composed of the experimental samples. Fitting these data requires three steps:

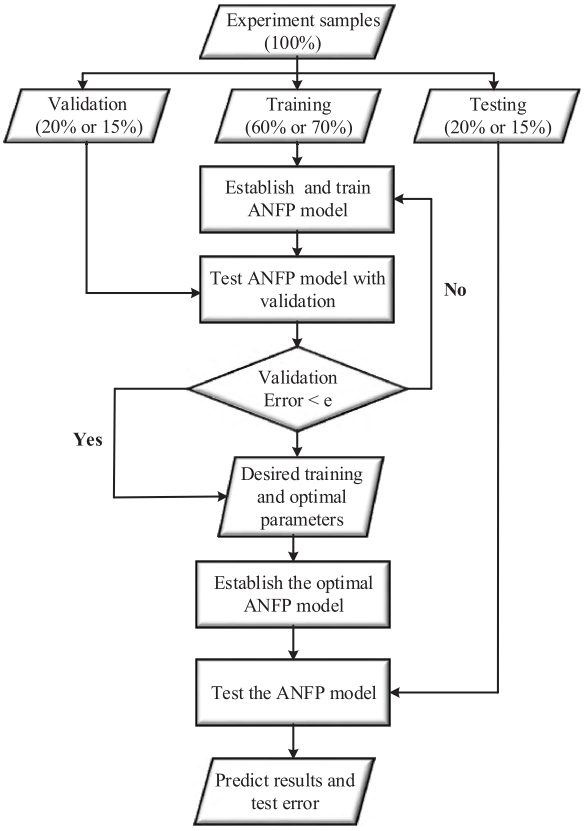

FIGURE 14. The scheme structure of input-output and curve fitting.

1 Twenty percent or fifteen percent of the data comprise the validation data. the sixty percent or seventy percent of the data comprise the training data. The remaining data are the testing data.

2 Establish and train the ANFP control model, and test the validation.

3 The optimal result is obtained when the validation error is smaller than e. The optimal ANFP model is established; thus, so the predicting results and testing errors are proposed.

- Case 1

There are two diverse stages and unique training data, validation data and testing data are shown in Fig.15. Seventy percent of the data are the training data, fifteen percent of the data are the validation data and fifteen percent of the data are the testing data. The best performance of the error, MSE and R value is achieved according to the fifteen or twenty hidden neurons. The best validation performance is 1.5091e-05 at epoch 659 in Fig.16. The expressions of the MSE and R value are as follows:

- Correlation coefficient (R)

$$R = \frac{\sum_{i=1}^{k} [(obs_i - avg\,(obs_i))}{\sqrt{\sum_{i=1}^{k} (obs_i - avg\,(obs_i))^2}} \times \frac{(pred_i - avg\,(pred_i))]}{\sum_{i=1}^{k} (pred_i - avg\,(pred_i))^2} \quad (16)$$

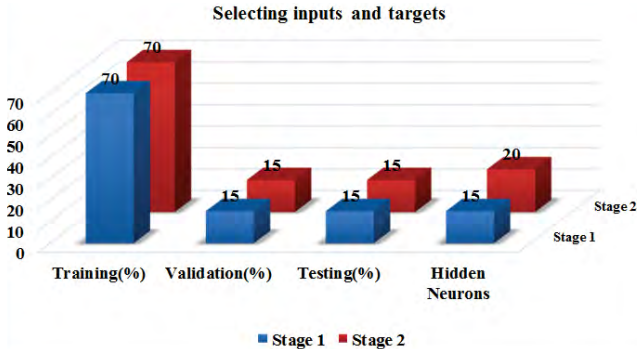

FIGURE 15. The selecting inputs and targets of case 1.

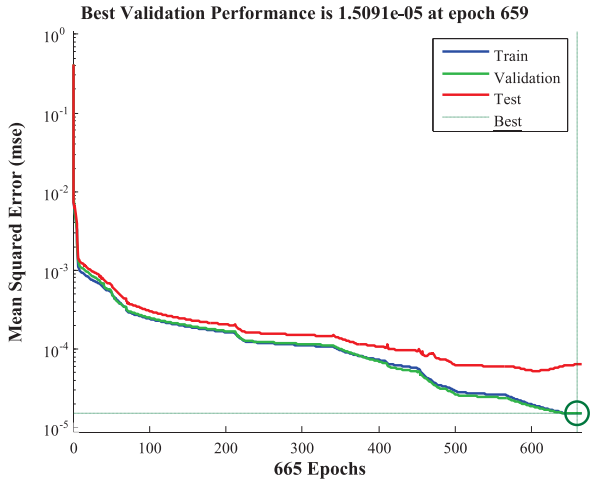

FIGURE 16. The mean squared error presentation in the stage 1 of case 1.

- Mean squared error (MSE)

$$\mathrm{MSE} = \sum_{i=1}^{n} \frac{\left(\exp_i - pred_i\right)^2}{n} \tag{17}$$

The ANFP model is trained by applying the nnstart toolbox of MATLAB. The MSE of the output coordinates is depicted according to the Levenberg-Marquardt (LM) algorithm. It is that The 0.000015091 targeted error values will be content to the demanding of the ANFP model training.

The normalized error histogram of neural network regression is presented in Fig.17. The errors (the difference between the targets and outputs) are slightly, that is to say, the predicted values approach to the real values.

The soft computing results of stage 1 are shown in Fig.18. The MSE measures are applied to evaluate the performance of the ANFP model in the training process. However, four input neurons, fifteen hidden neurons, and one output neuron are determined for the best ANFP model. By Using this model, the obtained performance measures are as follows: the MSE values are 0.0712%, 0.054% and 0.0867% for the training data, validation data and testing data, respectively. The R values of the ANFP model are 0.99697, 0.9717 and 0. 96655 for the training data, validation data and testing data, respectively.

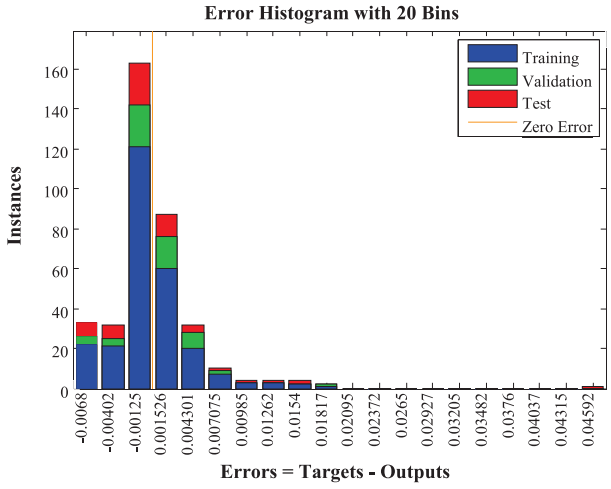

FIGURE 17. The error histogram in the stage 1 of case 1.

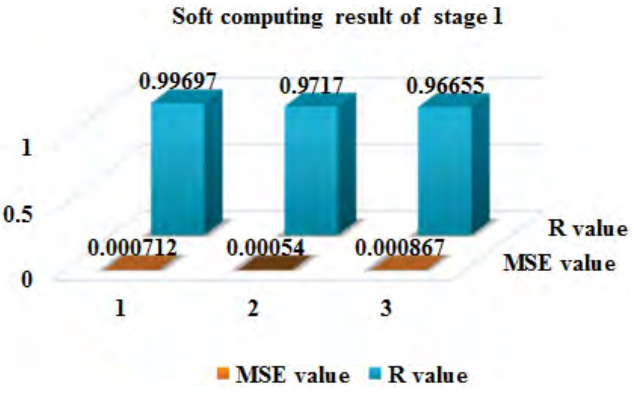

FIGURE 18. The soft computing result in the stage 1 of case 1.

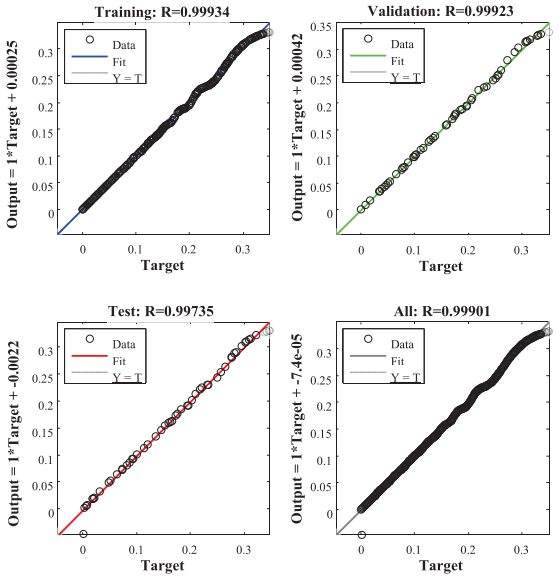

FIGURE 19. The structure of ANFP control training data in the stage 1 of case 1.

The target and output values of the ANFP model are computed in Fig.19. The LM training function is constructed as the training algorithm. Data that belong to the 372 trials are

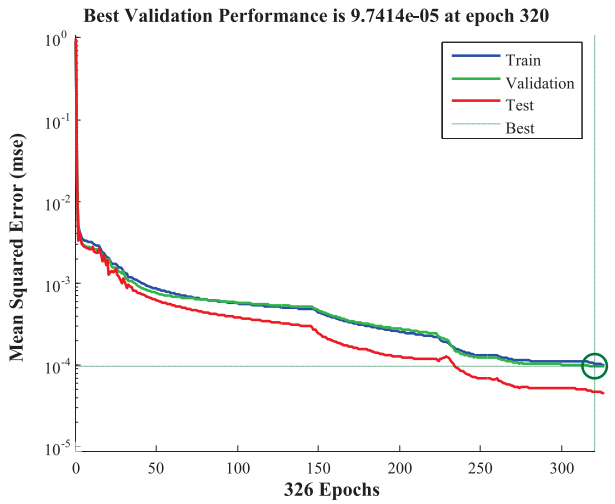

FIGURE 20. The mean squared error presentation in the stage 2 of case 1.

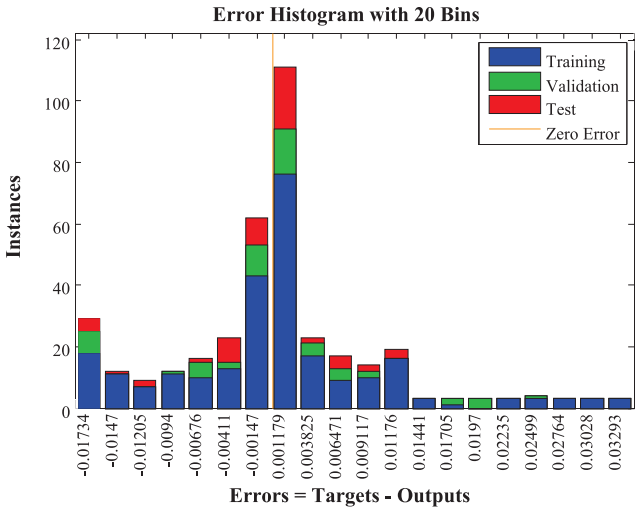

FIGURE 21. The error histogram in the stage 2 of case 1.

employed as follows: training: 70% (260) of the total trials; validation: 15% (56) of the total trials; and testing: 15% (56) of the total trials; and 15 hidden neurons of the ANFP model.

The soft computing results of stage 2: training, validation, testing, and hidden neurons are 70%, 15%, 15% and 20, respectively.

The ANFP is trained by the NN start toolbox. The MSE measures are presented according to the LM algorithm. The results of the training, validation, and testing data are consistent in the best results. The best validation performance is 0.000097414 at 320 epochs, which can satisfy the requirements of the ANFP training. The plot of MSE is indicated in Fig.20.

The histogram of normalized error for neural network regression is depicted in Fig.21. The errors (the difference between targets and outputs) are slightly, and the predicted values approach to the real values.

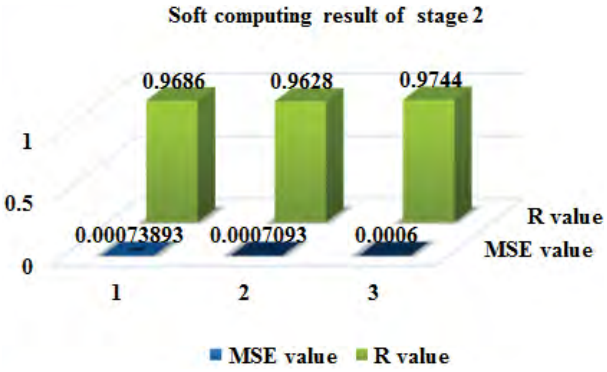

FIGURE 22. The soft computing result in the stage 2 of case 1.

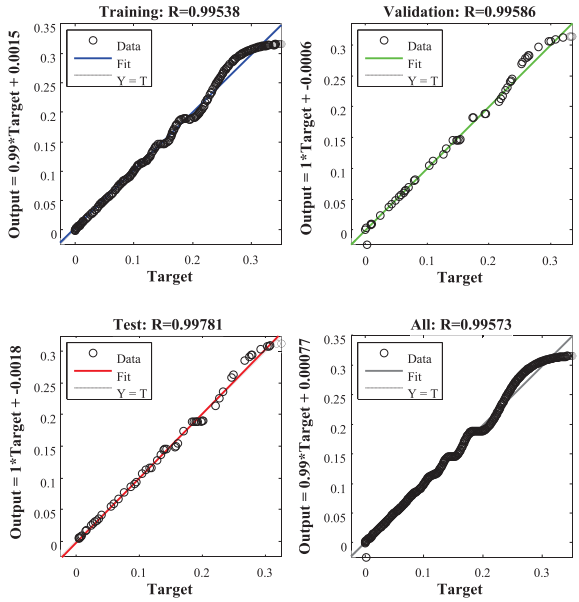

FIGURE 23. The structure of ANFP control training data in the stage 2 of case 1.

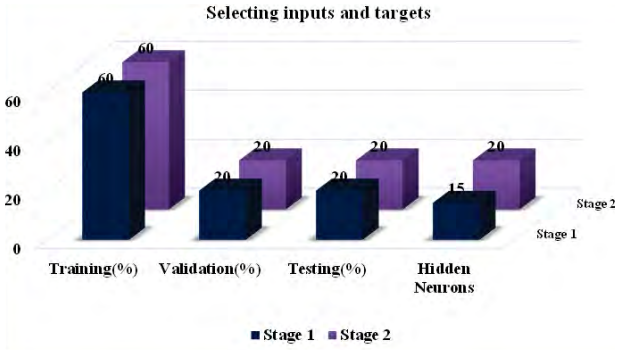

FIGURE 24. The selecting inputs and targets of case 2.

The soft computing values of stage 2 are shown in Fig.22, and the MSE results are applied to test the performance of the ANFP in the training process. However, four input neurons, twenty hidden neurons, and one output neuron are formulated in the best ANFP model. The obtained performance measures

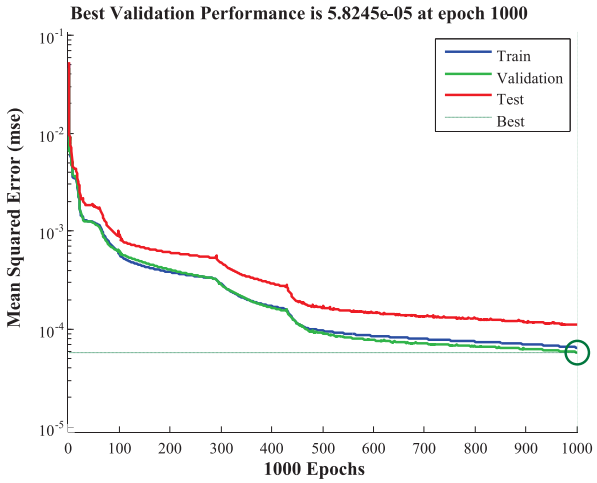

FIGURE 25. The mean squared error presentation in the stage 1 of case 2.

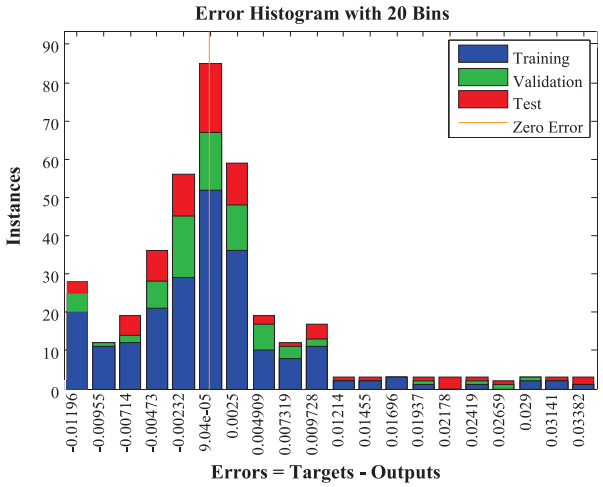

FIGURE 26. The error histogram in the stage 1 of case 2.

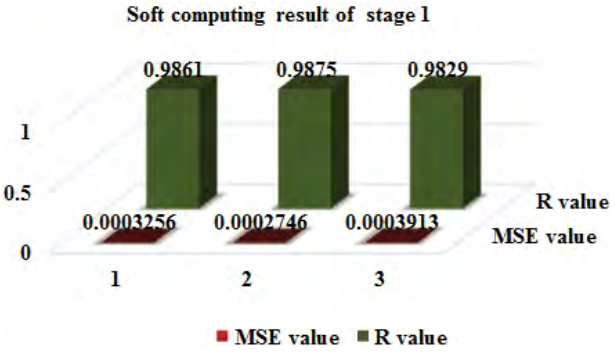

FIGURE 27. The soft computing result in the stage 1 of case 2.

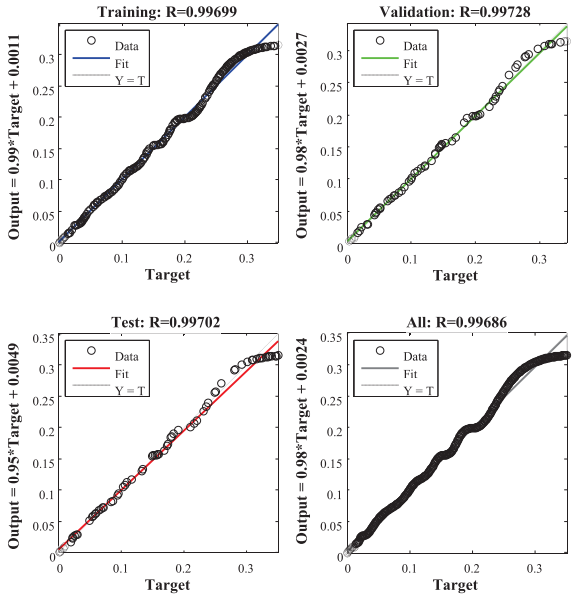

FIGURE 28. The structure of ANFP control training data in the stage 1 of case 2.

are as follows: the MSE values are 0.073893%, 0.07093% and 0.06%, and the R values of the ANFP model are 0.9686, 0.9628 and 0. 9744 for the training data, validation data and testing data, respectively. The targets and output values of the ANFP model are computed in Fig.23. The LM training function is adopted as the training algorithm. Data that belong to the 372 trials are employed for training: 70% (260) of the total trials validating: 15% (56) of the total trials, and testing: 15% (56) and 20 hidden neurons of the total trials of ANFP.

- Case 2

The training, validation, testing and hidden neurons are designed respectively according to the diverse hidden neurons, which form two stages. The details are demonstrated in Fig.24.

The training, validation, testing and hidden neurons are 60%, 20%, 20% and 15, respectively, in Fig.25.

The histogram of normalized errors for neural network regression is depicted in Fig.26. The errors (the difference between targets and outputs) is slightly, that is to say, the predicted values approach to the real values.

The soft computing values of stage 1 of the second simulation are introduced in Fig.27, and the mean squared error (MSE) measures are applied to examine the performance of the ANFP model in the training process. However, four input neurons, fifteen hidden neurons, and one output neuron are resolved for the best ANFP model. The obtained performance measures are as follows: the MSE values are 0.03256%, 0.02746% and 0.03913%; and the R values of the ANFP model are 0.9861, 0.9875 and 0. 9829 for the training data, validation data and testing data, respectively. As is shown in Fig.28, the values of the outputs of ANFP and the target values of the test data are computed. The LM training function is utilized as the training algorithm. The 372 data trials are employed as follows: training, 60 % (224) of total trials; validation, 20 % (74) of the total trials; testing, 20 % (74) of the total trials and 15 hidden neurons of the total trials of ANFP.

TABLE 2. Comparison result of controller performance.

Criteria	ANFP controller			Fuzzy-PID controller		
	Training	Validation	Testing	Training	Validation	Testing
MSE value	1.29E-08	1.028E-08	0.998E-08	0.000326	0.000275	0.00039
R value	0.999913	0.999925	0.999929	0.9861	0.9875	0.9829

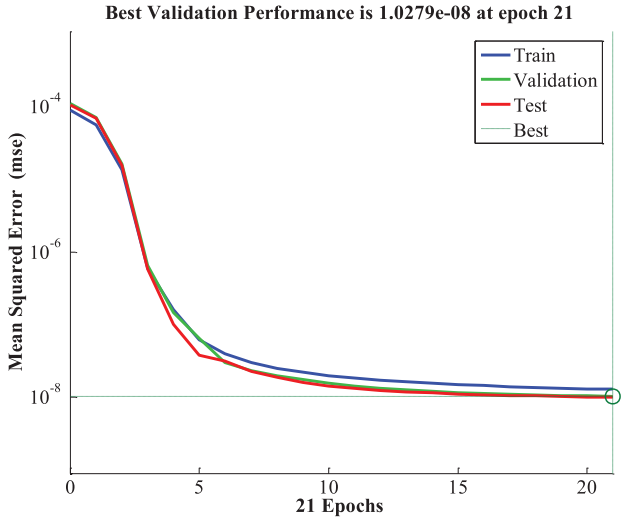

FIGURE 29. The mean squared error presentation in the stage 2 of case 2.

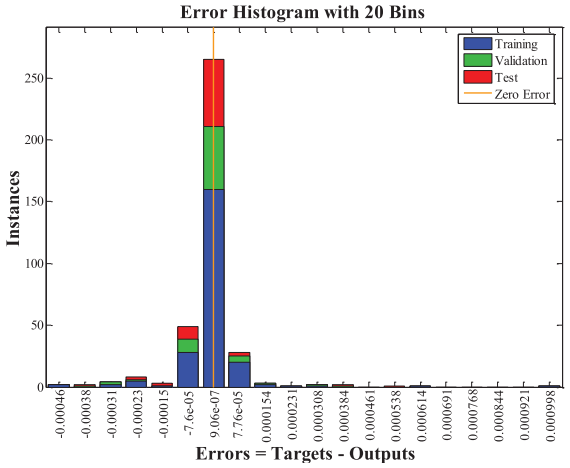

FIGURE 30. The error histogram in the stage 2 of case 2.

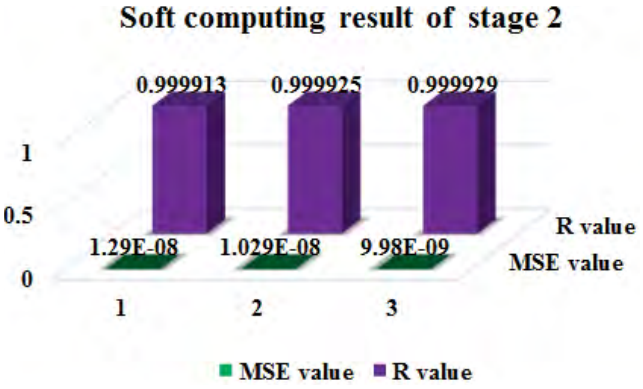

FIGURE 31. The soft computing result in the stage 2 of case 2.

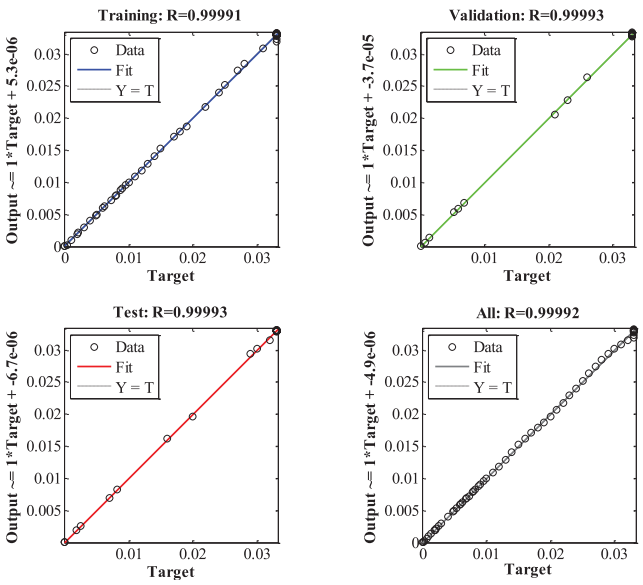

FIGURE 32. The structure of ANFP control training data in the stage 2 of case 2.

The training, validation, testing, and hidden neurons are 60%, 20%, 20% and 20 respectively, which form two stages.

An MSE chart of the output under by LM algorithm is shown in Fig.29. The results of training and testing are coincidence with the validation and the best values respectively. The best validation performance is 1.028E-08 at 21 epochs, which completely satisfy the testing targets.

The histogram of normalized error for neural network regression is depicted in Fig.30. The errors (the difference between targets and outputs) are smaller, that is to say, the predicted values approach to the real values.

The soft computing results of stage 2 of the second simulation are shown in Fig.31, and the MSE measures are applied to evaluate the performance of the ANFP model in the training process. However, four input neurons, fifteen hidden neurons, and one output neuron were determined for the best ANFP model. By Using this model, the obtained performance measures are as follows: the MSE values are 1.29E-08, 1.028E-08 and 0.998E-08, and the R values of the ANFP model are 0.999913, 0.999925 and 0.999929 for the training data, validation data and testing data respectively. The detailed comparative results are detailed in Table 2. As is shown in Fig.32, the values of the outputs of the

ANFP model and the target values of the test data are computed. The LM training function is utilized as the training algorithm. Data that belong to the 372 trials are employed as follows: training: 60% (224) of total trials; validation: 20% (74) of total trials; testing: 20% (74) of the total trials; and 20 hidden neurons of the total trials of ANFP.

VI. CONCLUSION

An adaptive neuro fuzzy PID control scheme is proposed to predict the performance of the controller outputs. The results of the outputs were trained and tested with the analytical results obtained from the outputs of ANFP control.

The predicting performance of the proposed controller output is illustrated by the mean squared error (MSE) and the coefficient of determination (R) as performance indicators. The prediction capabilities of the proposed controller have also been compared to the conventional fuzzy PID controller. The MSE values 1.29E-06%, 1.028E-06% and 0.998E-06% of ANFP are smaller than 0.0712%, 0.054%, 0.0867%, 0.073893%, 0.07093%, 0.06%, 0.03256%, 0.02746%, 0.03913%, respectively. Moreover, The MSE values of the ANFP controller are smaller than the MSE values of the other controllers. The R values of the ANFP model shows the excellent performance of the statistical results; the data have a better fitting effect. The experimental results validate the efficacy of the proposed model, which has the superiority of adaptability and robustness over classical methods.

REFERENCES

[1] J. M. Hilkert, "Inertially stabilized platform technology concepts and principles," *IEEE Control Syst.*, vol. 28, no. 1, pp. 26–46, Feb. 2008.

[2] P. J. Kennedy and R. L. Kennedy, "Direct versus indirect line of sight (LOS) stabilization," *IEEE Trans. Control Syst. Technol.*, vol. 11, no. 1, pp. 3–15, Jan. 2003.

[3] D. Li, H. Zhang, and Z. Yan, "Research on modeling and simulation for pitch/roll two-axis strapdown stabilization platform," in *Proc. Int. Conf. Electron. Meas. Instrum.*, 2011, pp. 42–46.

[4] H. Liao *et al.*, "Dynamics analysis and decoupling control for a differential cable drive inertially stabilized platform," *Proc. Inst. Mech. Eng. I, J. Syst. Control Eng.*, vol. 229, no. 7, pp. 652–661, 2015.

[5] F. Dong, X. Lei, and W. Chou, "A dynamic model and control method for a two-axis inertially stabilized platform," *IEEE Trans. Ind. Electron.*, vol. 64, no. 1, pp. 432–439, Jan. 2017.

[6] H. Yang *et al.*, "Study on the friction torque test and identification algorithm for gimbal axis of an inertial stabilized platform," *Proc. Inst. Mech. Eng. G, J. Aerosp. Eng.*, vol. 303, no. 10, pp. 66–79, 2015.

[7] R. Kumar and S. Kumar, "Performance analysis of robust controllers for inertially stabilized platform," *Int. J. Appl. Eng. Res.*, vol. 10, no. 14, pp. 33924–33928, 2015.

[8] A. A. Roshdy *et al.*, "Design a robust PI controller for line of sight stabilization system," *Int. J. Mod. Eng. Res.*, vol. 2, no. 2, pp. 144–148, 2012.

[9] A. K. Gaur *et al.*, "Fuzzy controller design for inertially stabilised platform," in *Proc. Found. Comput. Sci. (FCS)*, 2012, pp. 5–10.

[10] Y.-J. Liu and S. Tong, "Adaptive fuzzy control for a class of unknown nonlinear dynamical systems," *Fuzzy Sets Syst.*, vol. 263, pp. 49–70, Mar. 2015.

[11] E. Segredo, C. Segura, C. León, and E. Hart, "A fuzzy logic controller applied to a diversity-based multi-objective evolutionary algorithm for single-objective optimisation," *Soft Comput.*, vol. 19, no. 10, pp. 2927–2945, 2015.

[12] D. S. Bhandare and N. R. Kulkarni, "Performances evaluation and comparison of PID controller and fuzzy logic controller for process liquid level control," in *Proc. Int. Conf. Control, Autom. Syst.*, 2015, pp. 1347–1352.

[13] N. E. L. Y. Kouba, M. Menaa, M. Hasni, and M. Boudour, "Load frequency control in multi-area power system based on fuzzy logic-PID controller," in *Proc. IEEE Int. Conf. Smart Energy Grid Eng.*, Aug. 2015, pp. 1–6.

[14] M. A. Shamseldin and A. A. El-Samahy, "Speed control of BLDC motor by using PID control and self-tuning fuzzy PID controller," in *Proc. Int. Workshop Res. Edu. Mechatronics*, 2014, pp. 1–9

[15] C. Deng, S. Q. Xie, J. Wu, and X. Y. Shao, "Position error compensation of semi-closed loop servo system using support vector regression and fuzzy PID control," *Int. J. Adv. Manuf. Technol.*, vol. 71, no. 5, pp. 887–898, 2014.

[16] M. M. Ghiasi, M. Arabloo, A. H. Mohammadi, and T. Barghi, "Application of ANFIS soft computing technique in modeling the CO_2 capture with MEA, DEA, and TEA aqueous solutions," *Int. J. Greenhouse Gas Control*, vol. 49, pp. 47–54, Jun. 2016.

[17] S. Thomas, G. N. Pillai, K. Pal, and P. Jagtap, "Prediction of ground motion parameters using randomized ANFIS (RANFIS)," *Appl. Soft Comput.*, vol. 40, pp. 624–634, Mar. 2016.

[18] W. Phootrakornchai and S. Jiriwibhakorn, "Online critical clearing time estimation using an adaptive neuro-fuzzy inference system (ANFIS)," *Int. J. Elect. Power Energy Syst.*, vol. 73, pp. 170–181, Dec. 2015.

[19] L.-Y. Wei, "A hybrid ANFIS model based on empirical mode decomposition for stock time series forecasting," *Appl. Soft Comput.*, vol. 42, pp. 368–376, May 2016.

[20] S. Prakash and S. K. Sinha, "Simulation based neuro-fuzzy hybrid intelligent PI control approach in four-area load frequency control of interconnected power system," *Appl. Soft Comput.*, vol. 23, no. 5, pp. 152–164, 2014.

[21] H. R. do N. Costa and A. La Neve, "Study on application of a neuro-fuzzy models in air conditioning systems," *Soft Comput.*, vol. 19, no. 4, pp. 929–937, 2015.

[22] M. Sridevi, P. Prakasam, and P. M. Sarma, "Model identification of non linear systems using soft computing technique," in *Proc. IEEE Adv. Comput. Conf.*, Feb. 2014, pp. 1174–1178.

[23] M. A. Dena, F. Palis, and A. Zeghbib, "Modeling and control of non-linear systems using soft computing techniques," *Appl. Soft Comput.*, vol. 7, no. 3, pp. 728–738, 2007.

FENG LIU received the master's degree in numerical mathematics from Yan Shan University, China, in 2013. He is currently pursuing the Ph.D. degree with the School of Astronautics, Beihang University, China. His research interests include aerospace engineering, flight vehicle design, UAV design, control engineering, neural networks, and intelligent control scheme.

HUA WANG received the Ph.D. degree from the Beijing Institute of Technology. He is currently a Professor with Beihang University. His research interests include the new concept of micro and small craft technology research and shells that contain miniature aircraft system design and analysis.

QINGLI SHI received the bachelor's degree from the School of Astronautics, Beihang University, in 2015. He is currently pursuing the Ph.D. degree in aircraft design with the School of Astronautics, Beihang University, under the supervision of Prof. W. Hua. His research interests include the collective design of several unmanned aircraft vehicles and genetic algorithm. He is currently researching an optimal design based on a genetic algorithm for a UAV with inflatable wings.

HENGXIAN WANG received the bachelor's degree in ammunition engineering and explosion technology from the North University of China in 2016. He is currently pursuing the master's degree with Beihang University. His research interests include system design of the aircraft and control engineering.

MENGYING ZHANG received the B.Eng. degree in measuring and control technology and instrumentations from the Huazhong University of Science and Technology, China, in 2016. She is currently pursuing the master's degree in aeronautical and astronautical science and technology, Beihang University, China. Her research interests include the implementation and application of control algorithms in unmanned multi-rotor aircrafts.

HAILONG ZHAO received the bachelor's degree from the North University of China and the master's degree in aerospace science and technology from the Beijing University of Aeronautics and Astronautics, in 2010 and 2015, respectively. He studied the flight vehicle design and UAV design.